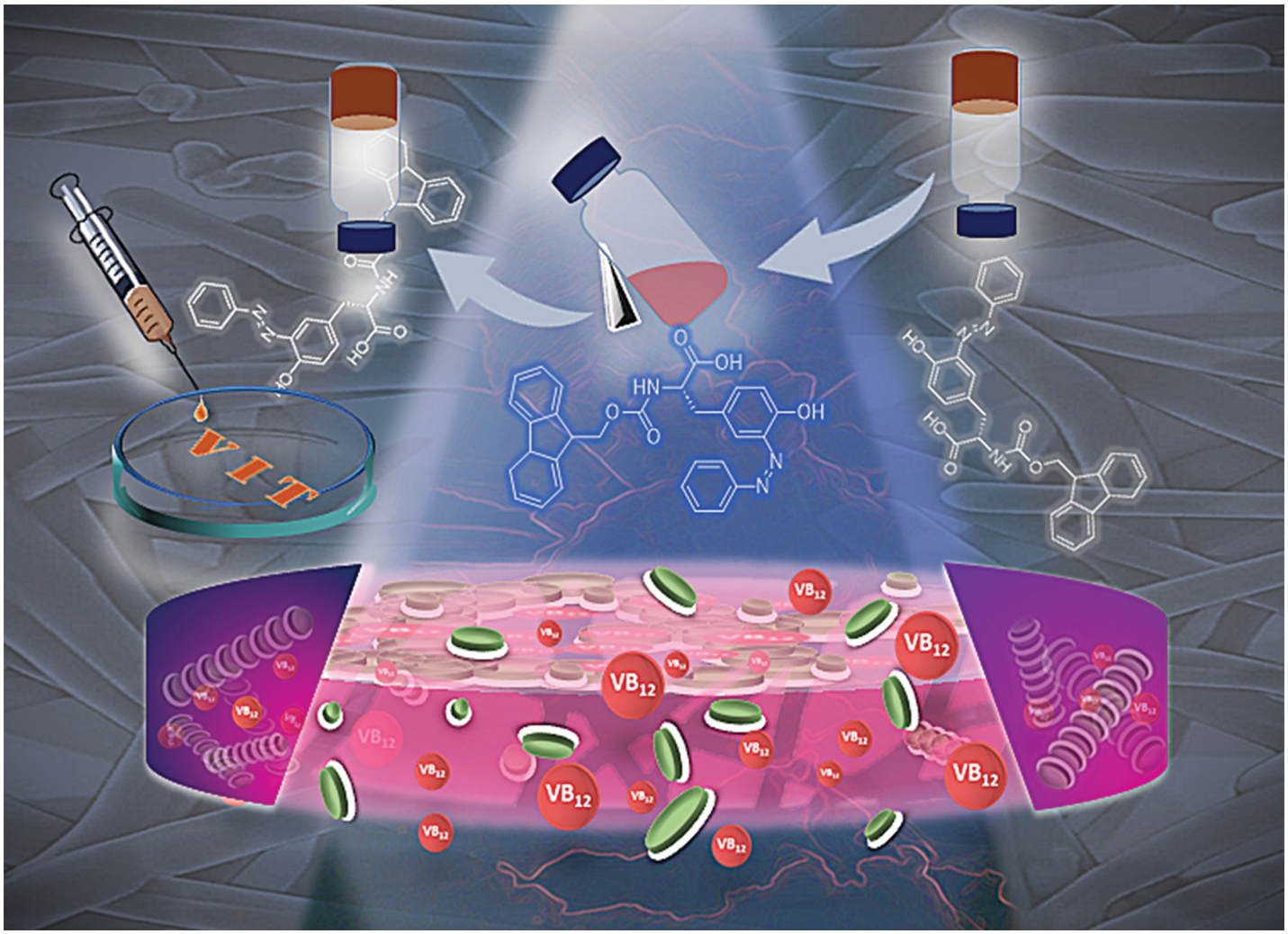


**Showcasing research from Dr Chandan Maity's (Organic) Material Science and Engineering Laboratory, Centre of Nanobiotechnology, Vellore Institute of Technology, Vellore Campus, Tamil Nadu, India.**

A light responsive single amino acid-based supramolecular hydrogel for photo-controlled vitamin release

This work introduces a light-responsive, low-molecular-weight hydrogelator (FmocY-Azo) as a versatile platform for controlled therapeutic delivery. Derived from tyrosine and incorporating an azobenzene photoswitch, FmocY-Azo self-assembles under ambient conditions into a supramolecular fibrous hydrogel. The material exhibits thixotropy and dual thermal–photo responsiveness. The material effectively encapsulates vitamin $B_{12}$ and enables on-demand release upon light irradiation *via* photoinduced network restructuring. Release follows Korsmeyer–Peppas kinetics under light and zero-order behaviour in the dark, highlighting its potential for precise, light-triggered therapeutic delivery.

Image reproduced by permission of Divya Chauhan and Chandan Maity from *Mater. Adv.*, 2026, **7**, 175.

## As featured in:


See Divya Chauhan and Chandan Maity, *Mater. Adv.*, 2026, **7**, 175.

ROYAL SOCIETY OF CHEMISTRY

rsc.li/materials-advances

Registered charity number: 207890

Materials Advances

ROYAL SOCIETY OF CHEMISTRY

COMMUNICATION

View Article Online
View Journal | View Issue



Cite this: *Mater. Adv.*, 2026, 7, 175

Received 9th July 2025,
Accepted 6th November 2025

DOI: 10.1039/d5ma00736d

rsc.li/materials-advances

# A light responsive single amino acid-based supramolecular hydrogel for photo-controlled vitamin release

Divya Chauhan and Chandan Maity *

**Light responsive low-molecular-weight hydrogelators (LMWHs) offer a promising platform for controlled delivery applications *via* light triggered structural changes in the hydrogel network. In this study, we report the facile synthesis of a tyrosine-derived LMWH, FmocY-Azo, incorporating a photoresponsive azobenzene moiety. Self-assembly of FmocY-Azo under ambient conditions provides the supramolecular hydrogel material that displays thixotropic behavior, as well as thermal and light responsiveness. The hydrogel material effectively encapsulates vitamin $B_{12}$ within its fibrous network and enables its controlled release upon light irradiation, driven by structural changes in the FmocY-Azo framework. The release kinetics follows the Korsmeyer–Peppas model in the presence of light irradiation, whereas it follows zero-order kinetics in the dark, indicating a combined effect of diffusion and light-induced network disassembly. This work presents a single amino acid-based light responsive fibrous hydrogel with potential for developing light-triggered drug delivery systems.**



## 1. Introduction

Molecular self-assembly is a fundamental process that plays a crucial role in the formation of complex structures in natural systems utilising noncovalent interactions such as hydrogen bonding, π–π stacking, van der Waals forces, and electrostatic interactions. Spontaneous self-assembly of molecular precursors enables the emergence of intricate architectures with remarkable structural complexity and functional capabilities.[1,2] Inspired by the natural self-assembly process, artificial supramolecular materials have been developed for their use in biology, nanotechnology and medicine. Among these, hydrogels have emerged as an emerging class of materials due to their broad applicability in areas such as tissue engineering, controlled drug delivery, bioimaging, and biosensing.[3–6] Hydrogel materials formed by low molecular weight hydrogelators (LMWHs) are particularly fascinating as the self-assembly of small molecules resulted in one-dimensional supramolecular chains that form a hydrogel network entrapping a large amount of water.[7,8] Among recently developed LMWH-based platforms, the self-assembly of amino acids or their derivatives has garnered significant attention as amino acids are the simplest structural elements in biological systems that can serve as the building blocks for complex molecular architectures, and can be synthesized or derivatized with high scalability.[9–12] Thus, single amino acid-based supramolecular systems have been extensively explored from the biological field to nanotechnology due to their ready availability, biocompatibility, and biodegradability.

Stimuli-responsive hydrogel materials represent "smart" materials that can undergo a physicochemical transition in response to stimuli such as changes in pH, temperature changes, light irradiation, and the presence of enzymes or specific biomolecules.[13–18] Thus, the development of these smart materials offers control over the material properties in response to the presence/absence of stimuli. Among these stimuli, light irradiation for the physicochemical change of hydrogel materials is advantageous over other stimuli as light can be applied spatiotemporally with great ease and convenience with other tuneable parameters such as intensity and duration.[5,19,20] Light-responsive LMWHs generally consist of a photochromic unit, such as azobenzene, stilbene, coumarins, and spiropyran, that is responsible for structural transformations, such as isomerisation, tautomerisation or ring closure/opening.[21–26] Light irradiation typically leads to structural changes in LMWHs, resulting in hydrogel → sol conversion, which can lead to the release of entrapped therapeutics, such as drug molecules, proteins, and vitamins.[27,28] Among them, controlled release of vitamins such as vitamin $B_{12}$ ($VB_{12}$) is crucial for optimizing their therapeutic efficacy and minimizing potential side effects.[29] However, the majority of light-responsive supramolecular hydrogel systems are based on

*(Organic)Material Science and Engineering Laboratory, Center for Nanobiotechnology (CNBT), Vellore Institute of Technology, Vellore Campus, Tamil Nadu, 632014, India. E-mail: chandanmaitylab@gmail.com, chandan.maity@vit.ac.in*

peptide-derived LMWHs conjugated with photochromic moieties and often suffer from multi-step synthesis and/or complex purification steps.[30,31] Moreover, hydrogel formation is often achieved through a heating–cooling process, which can be unreliable for the biological environments. On the other hand, single amino acid-based light responsive hydrogel systems are nearly absent from the literature.[32,33] Therefore, the development of light-responsive supramolecular hydrogel materials that can be obtained under ambient conditions from easily available amino acid-based LMWHs remains a significant challenge.

Here, we report one-pot synthesis of a tyrosine-based LMWH (FmocY-Azo, Fig. 1a) consisting of an azobenzene moiety for the formation of a light-responsive hydrogel matrix. Self-assembly of FmocY-Azo under ambient conditions provides the hydrogel material (Fig. 1a, top panel). Light irradiation results in hydrogel → sol conversion due to *trans* → *cis* structural isomerization of the azobenzene moiety. The hydrogel material also displays thixotropic behaviour and thermal responsiveness. In addition, $VB_{12}$ (as a therapeutic) is incorporated within the hydrogel network for light-triggered controlled release (Fig. 1a, bottom panel). Thus, precise modulation of the release of desired therapeutics is possible *via* the application of the light stimulus from a hydrogel matrix that can be obtained under ambient conditions from easily accessible materials.

# 2. Experimental

## 2.1 Materials

All the chemical reagents and solvents were used as received from the commercial sources without further purification. Fmoc-tyrosine (FmocY 95%) and hydrochloric acid (HCl, 32%) were purchased from Avra Synthesis Pvt Ltd. Sodium nitrite ($NaNO_2$) was purchased from Spectrochem Pvt Ltd, Mumbai. Aniline, acetonitrile, and vitamin $B_{12}$ were purchased from SRL, India. DMSO-$d_6$ was obtained from Sigma-Aldrich.

## 2.2 Methods

**Synthesis of FmocY-Azo.** Concentrated HCl (1.5 mL) was added dropwise to a mixture of aniline (0.93 mL, 12.0 mmol) in distilled water (10.0 mL) at 0 °C. $NaNO_2$ (0.77 g, 12.0 mmol) was added to the mixture at this temperature, and it was stirred for 30 minutes. Next, the mixture was slowly added to a flask containing a mixture of FmocY (2.15 g, 10.7 mmol) in acetonitrile (25.0 mL), and $NaHCO_3$ (1.20 g, 10.7 mmol) in distilled water (30.0 mL) at 0 °C. Afterward, the mixture was allowed to reach ambient temperature and stirred for 24 h. The resulting dark red mixture was diluted with distilled water (50.0 mL) and extracted with ethyl acetate (EtOAc, 50.0 mL × 3 times). The organic layers were combined and washed with water (50.0 mL × 2 times) and brine (50.0 mL × 2 times). The organic layer was then dried over anhydrous $Na_2SO_4$ and concentrated

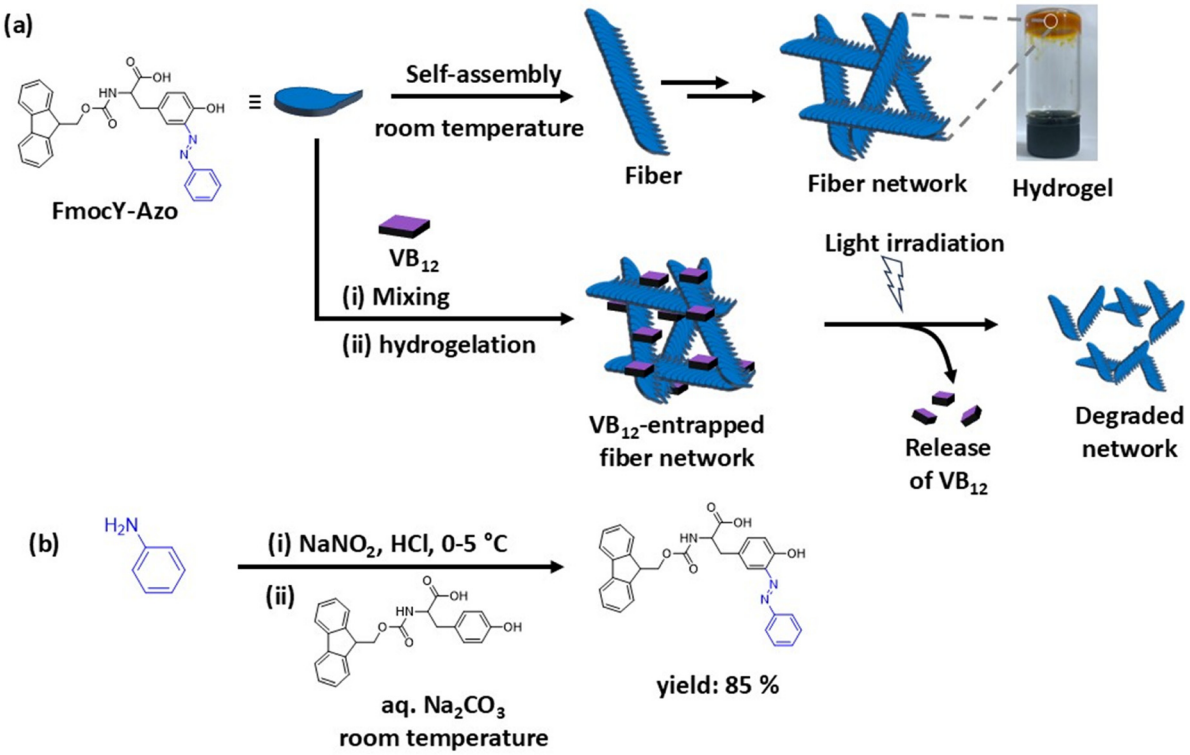


Fig. 1 Light responsive hydrogel. (a) A schematic of light-responsive hydrogel material preparation *via* self-assembly of FmocY-Azo (top panel), and entrapment of $VB_{12}$ within the hydrogel matrix that allow light-induced controlled release of $VB_{12}$ (bottom panel), (b) synthetic steps for the preparation of FmocY-Azo.

under reduced pressure using a rotary evaporator, yielding a red solid, which was purified using column chromatography with EtOAc and hexane (EtOAc/hexane = 7 : 3) as the eluent. FmocY-Azo was obtained as a red solid (4.73 g, 85%). $^1$H NMR (400 MHz, DMSO-$d_6$): $\delta$ 9.16 (s, 1H), 7.81 (d, $J$ = 7.6 Hz, 2H), 7.67 (d, $J$ = 7.6 Hz, 1H), 7.59 (t, $J$ = 8.3 Hz, 3H), 7.44 (s, 1H), 7.33 (dd, $J$ = 7.5, 3.3 Hz, 2H), 7.24 (dt, $J$ = 10.5, 7.5 Hz, 2H), 6.97 (s, 1H), 6.93 (t, $J$ = 7.8 Hz, 1H), 6.59 (d, $J$ = 8.1 Hz, 2H), 6.48 (d, $J$ = 7.8 Hz, 1H), 6.04 (s, 1H), 4.04–3.94 (m, 2H), 2.89 (dd, $J$ = 13.8, 4.4 Hz, 1H), 2.68 (dd, $J$ = 13.8, 10.2 Hz, 1H), 1.92 (s, 1H), 1.16 (s, 1H), 1.10 (t, $J$ = 7.1 Hz, 1H). $^{13}$C NMR (100 MHz, DMSO-$d_6$): $\delta$ = 155.91, 155.85, 152.89, 152.47, 148.62, 143.77, 142.81, 140.68, 130.06, 129.41, 128.81, 128.07, 127.64, 127.08, 125.19, 121.72, 120.11, 115.63, 114.95, 113.87, 113.39, 65.60, 59.78, 55.97, 46.59, 35.79, 20.78, 14.10. IR (neat, $\nu$ cm$^{-1}$): 3371(–OH stretching), 1717 (C═O stretching), 1499 (–N═N– stretching), 1226 (–C–N stretching). HRMS (ESI, Pos. mode): $m/z$ calcd. for $C_{30}H_{25}N_3O_5$: exact mass 508.32; found 508.35.

**Preparation of the hydrogel and determination of minimum gelation concentration (MGC).** A stock solution of FmocY-Azo (250 mM) was prepared by dissolving FmocY-Azo (63.75 mg) in DMSO (0.5 mL). This stock solution was then added to 10 mM phosphate-buffered saline (PBS) to initiate hydrogel formation. The resulting mixture was gently mixed and left undisturbed under ambient conditions. Gelation was assessed using the vial inversion method.

**UV-vis study.** UV-vis spectroscopy was performed to investigate the pH-dependent behavior of FmocY-Azo over the pH range of 4.0 to 8.0 in phosphate buffer solution. A stock solution of FmocY-Azo in DMSO was diluted with PBS buffer in a 1 : 9 (v/v) ratio to prepare samples at the desired pH values. UV-vis spectra were recorded in the range of 200–800 nm at a fast scan rate.

**FTIR analysis.** For FTIR analysis, the hydrogel samples were prepared in PBS buffer at pH values of 4.0, 5.0, 6.0, and 7.0. For lyophilization, the samples were kept in a refrigerator for 24 hours, followed by lyophilization using a freeze-dryer.

**FE-SEM analysis.** Lyophilized FmocY-Azo hydrogel samples were sputter-coated with gold using a Quorum QT150S Plus coater and mounted on carbon stubs. The samples were imaged using a Thermo Fisher FEI QUANTA 250 FEG field-emission scanning electron microscope (FE-SEM) in secondary electron (SE) mode at an accelerating voltage of 20 kV. Images were acquired at 1000×, 5000×, 10 000×, and 15 000× magnifications.

**TEM analysis.** Samples for transmission electron microscopy (TEM) were prepared using the drop-casting method. Briefly, 20 μL of the FmocY-Azo solution in PBS buffer (pH 5.0) was carefully deposited onto carbon-coated copper TEM grids. After 5 minutes, excess liquid was gently blotted with filter paper, and the grids were allowed to dry under ambient conditions for 24 hours. The dried samples were then imaged using a transmission electron microscope.

**Thixotropic rheology analysis.** To monitor gel formation, a solution of FmocY-Azo in DMSO was added to PBS buffer (10 mM, pH 5.0), and the mixture was immediately transferred onto a Peltier plate rheometer maintained at 25 °C, with a 1 mm gap between the plates. A time sweep was conducted at a constant angular frequency of 6 rad s$^{-1}$ and a strain of 0.1% within the linear viscoelastic region of the material. Upon completion of gelation, the strain was increased to 50% for 10 minutes to disrupt the network, after which it was reduced back to 0.1% to monitor the recovery and reformation of the gel structure.

**Light-induced gel–sol transitions.** The light-induced hydrogel-to-sol transition was found to depend on several factors, including the hydrogelator concentration, the presence of vitamin $B_{12}$, light intensity, and the distance between the light source and the sample. All experiments were performed in multiple replicates and yielded consistent results under identical conditions. Hydrogels were prepared in PBS buffer (pH 5.0) using the solvent-switching method in 3.5 mL quartz cuvettes (Lark). The samples were then exposed to 370 nm light at ambient temperature, with the light source positioned 9.0 cm from the vial. Upon irradiation for a defined period, the hydrogel underwent a transition to the sol state without the need for mechanical agitation.

**Vitamin $B_{12}$ ($VB_{12}$) entrapped within the FmocY-Azo hydrogel.** $VB_{12}$-entrapped hydrogels were prepared by first mixing 20 μL of an aqueous $VB_{12}$ solution (0.1 mM) with a DMSO solution of FmocY-Azo. This mixture was then added to phosphate buffer (10 mM, pH 5.0 or pH 7.4) to a final volume of 1.0 mL, resulting in final FmocY-Azo concentrations of 6.0 mM (pH 5.0) and 7.8 mM (pH 7.4), respectively. The samples were left undisturbed at room temperature for approximately 120 minutes to allow self-assembly and hydrogel formation.

**Light-induced release of $VB_{12}$.** $VB_{12}$ release studies were conducted in PBS buffer. For each experiment, 1.7 mL of PBS was carefully added on top of the $VB_{12}$-loaded hydrogel prepared in a quartz cuvette. At predetermined time intervals, 1.0 mL aliquots were withdrawn from the supernatant without disturbing the gel and replaced with an equal volume of fresh PBS to maintain a constant volume. The concentration of $VB_{12}$ in each aliquot was quantified by UV-vis spectroscopy. For light-induced release studies, the same procedure was followed, with the $VB_{12}$-loaded hydrogel placed in an irradiation chamber and exposed to 370 nm light. The concentration of $VB_{12}$ in each aliquot was determined using a standard calibration curve. The calibration curve was constructed by plotting the absorbance of aqueous $VB_{12}$ solutions at 550 nm against known concentrations, prepared by serial dilution of a 5.0 mM $VB_{12}$ stock solution. The release rate of $VB_{12}$ was calculated using the following equation:

$$\text{Release of } VB_{12}\ (\%) = \frac{W_0}{W_t} \times 100$$

where $W_t$ is the amount of $VB_{12}$ encapsulated in the hydrogel sample and $W_0$ is the amount of released $VB_{12}$ after the light-irradiation step.

**Kinetic study for the release of $VB_{12}$.** The kinetic studies on the release of encapsulated $VB_{12}$ were carried out using the

following four models: zero-order model, first-order model, Higuchi model, and Korsmeyer–Peppas model.

$$\text{Zeroth-order model: } Q_t = k_0 t + Q_0$$

where $Q_t$ is the amount of drug dissolved at time $t$, $Q_0$ is the initial amount of $VB_{12}$ in the solution, and $K_0$ is the zero-order release constant.

$$\text{First-order model: } \log C = \log C_0 + \frac{kt}{2.303}$$

where $C_0$ is the initial concentration of $VB_{12}$, $K$ is the first-order rate constant, and $t$ is time.

$$\text{Higuchi model: } Q = K_H \sqrt{t}$$

where $Q$ is the amount of $VB_{12}$ released at time $t$ and $K_H$ is the Higuchi constant.

$$\text{Korsmeyer–Peppas model: } \log(M_t/M_\infty) = \log k + n \log t$$

where $M_t/M_\infty$ is the fraction of $VB_{12}$ released at time $t$, $K$ is the release rate constant and $n$ is the release exponent.

# 3. Results and discussion

## 3.1 Molecular design and synthesis

To design a novel light-responsive LMWH based on a single amino acid, we selected tyrosine due to its multifaceted role in biological processes such as signal transduction, enzyme catalysis, and protein interactions.[10,34] The aromatic side chain contributes to the stability and specificity of protein structures, whereas the phenolic hydroxyl group is a key site for phosphorylation regulating various cellular activities. In addition, the fluorenylmethoxycarbonyl functionalized tyrosine derivative (FmocY) has been employed for the preparation of supramolecular hydrogel materials under ambient conditions *via* the solvent-switching method utilising hydrogen bonding and π–π stacking interactions.[12,35,36] Aiming to develop a photo-responsive LMWH, we designed a derivative of FmocY by conjugating the azobenzene moiety as a light-responsive unit at the *ortho*-position of the phenolic –OH group. The resulting FmocY-Azo was synthesized in good yield *via* the formation of benzene diazonium chloride, followed by reaction with the phenol moiety of FmocY (Fig. 1b). The compound FmocY-Azo was characterised using $^1$H NMR, $^{13}$C NMR, mass, HPLC and IR spectroscopic techniques (Fig. S1–S5).

## 3.2 Light-responsiveness of FmocY-Azo

UV-vis spectroscopic analysis of FmocY-Azo in dimethyl sulfoxide (DMSO) was conducted and compared with that of FmocY (Fig. S6). In comparison to the absorption spectra of FmocY, the appearance of an additional absorption peak at 354 nm in FmocY-Azo confirmed the successful incorporation of the azobenzene moiety. The photoswitching behaviour of FmocY-Azo (Fig. 2a) was evaluated by

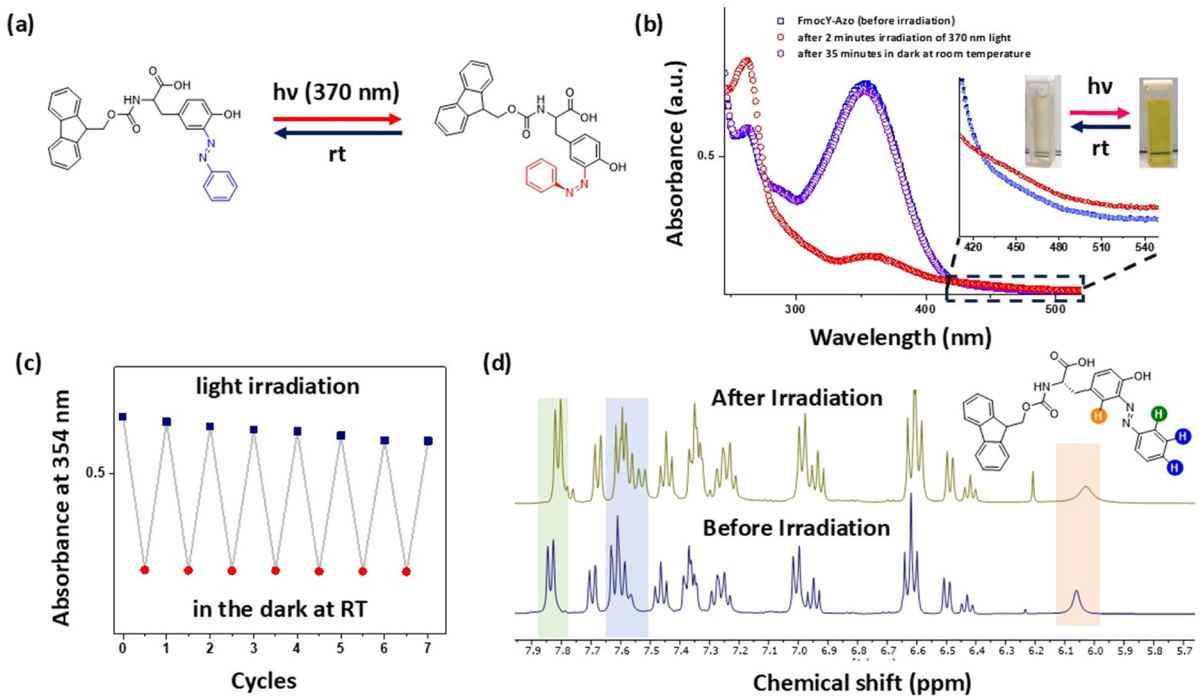


Fig. 2 Photoswitching of FmocY-Azo: (a) chemical structures of the *trans*- and *cis*-isomers of FmocY-Azo, (b) UV-vis absorption spectra in DMSO of FmocY-Azo ($5 \times 10^{-5}$ M) before light irradiation (blue square), upon irradiation with 370 nm light for 2 minutes (red circle), and after keeping in the dark at room temperature for 35 minutes (light blue triangle) (inset: a solution of FmocY-Azi in DMSO before and after irradiation with 370 nm light), (c) reversible switching of absorption in DMSO monitored at 354 nm upon irradiation with 370 nm light (indicated with blue circle) and thermal back-reaction at room temperature in the dark (indicated with red circle), and (d) partial $^1$H NMR (400 MHz, DMSO-$d_6$) spectra of FmocY-Azo (as prepared, bottom panel) and after irradiation with 370 nm light (top panel).

UV-vis and NMR spectroscopy. Irradiation of FmocY-Azo in DMSO with 370 nm light for ~2 minutes under ambient conditions provided the photostationary state enriching *cis*-isomer (Fig. 2b, red circle). It is worth mentioning that light irradiation was performed at room temperature in a photoreactor with integrated cooling fans to maintain ambient conditions.

Irradiation with light led to a decrease in absorption at 354 nm, accompanied by slight increases at 260 nm and 450 nm. This change is attributed to the disruption of the π–π* transition of the *trans*-isomer and the emergence of the n–π* transition characteristics of the *cis*-isomer.[37] This spectral change is consistent with the observed colour shift of the solution from pale yellow to orange (Fig. 2b, inset), which arises due to the slightly red-shifted n–π* absorption band associated with the *cis*-isomer, exhibiting a characteristic absorption in the visible region around 450 nm.[38,39] Keeping the sample in the dark at room temperature, the original absorption spectra were recovered in ~35 minutes (Fig. 2b, blue triangle), indicating thermal back-isomerization (*cis* → *trans*) of FmocY-Azo.

Besides, reversible switching of FmocY-Azo *via* light induced *trans* → *cis* isomerization and subsequent thermal back-reaction to the *trans*-form was examined by following the absorbance at 354 nm, showing excellent photoswitching behaviour in DMSO (Fig. 2c). Likewise, FmocY-Azo exhibited comparable photoisomerization behaviour in nearly pure water (Fig. S7). UV-vis analysis revealed a reduction in the characteristic π → π* absorption band of FmocY-Azo at 354 nm, indicating aggregation of the molecules in the aqueous environment (*vide infra*). Under 370 nm irradiation, *trans* → *cis* conversion was significantly slower than in DMSO. Likewise, thermal *cis* → *trans* back-isomerization in the dark required ~50 minutes. This sluggish behaviour is presumably due to aggregation-induced restriction of intramolecular motion, which inhibits efficient photoisomerization.[40] Furthermore, $^1$H NMR was employed to substantiate the light-triggered isomerization of FmocY-Azo (Fig. 2d). Before light irradiation, the spectra (in DMSO-$d_6$) showed a stable *trans*-isomer, whereas irradiation with 370 nm light for 2 minutes displayed a photo-stationary state having *ca.* 65% *cis*-isomer. New up-field signals for core protons of the azobenzene moiety (shaded area) confirmed *trans* → *cis* isomerization. However, due to technical issues, NMR spectra were recorded after ~15-minute delay post-irradiation, resulting in only minimal observed chemical-shift changes. Collectively, UV-vis and NMR spectral data confirmed the reversible isomerization of FmocY-Azo upon light irradiation and its thermal reversion in the dark.

### 3.3 Hydrogelation of FmocY-Azo

UV-vis spectroscopic analysis was performed to investigate the effect of water on the self-assembly of FmocY-Azo. In pure DMSO, the spectrum displayed absorption bands between 250 and 400 nm, with sharp peaks at 260 nm and 354 nm (Fig. 3a), indicating the presence of the free monomer in DMSO. In contrast, a decrease in band intensity accompanied by a red shift of ~5 nm was observed in the aqueous solution of FmocY-Azo, indicating molecular assembly driven by π–π stacking interactions. Thereafter, hydrogelation of FmocY-Azo was investigated without light irradiation by the solvent switching method[12,41] under ambient conditions. Briefly, a solution of FmocY-Azo in DMSO (250 mM) was diluted with phosphate-buffered saline (PBS, 10.0 mM) at room temperature, gently mixed, and then left undisturbed for hydrogel formation (Fig. 3b). The minimum gelation concentration (MGC) was determined using the inverted tube test. MGC was the point between the last concentration at which the hydrogel was formed and the concentration at which the material could not support its own weight. Results showed that both gelation time and MGC were dependent on solution pH (Table S1). It required longer gelation times and higher MGC values for the solution of high pH—for example, gelation required 90 minutes with an MGC of 6.0 mM at pH = 7, whereas it required more than 2 hours with an MGC of 6.5 mM at pH = 8. Besides, the resulting hydrogel at basic pH was weak to support its own weight. In contrast, hydrogelation was observed within 45 minutes with an MGC of 5.0 mM at pH = 5 (Table S2).

The ionizable groups (–$CO_2$H and phenolic OH) present in FmocY-Azo that could be (de)protonated at different pH values may result in different pathways for self-assembly of FmocY-Azo.[42] To realize pH dependent hydrogelation, UV-vis spectra of FmocY-Azo were recorded in DMSO/PBS buffer (1 : 9) at different pH values (Fig. 3c). At acidic pH, the π–π* absorption band at 354 nm decreased, while the band at 260 nm increased, which indicated protonation of the azo group.[43] At pH 5, the absorption band at 260 nm decreased and the absorption band at 354 nm reappeared. At higher pH, deprotonation of FmocY-Azo generates carboxylate species, that induces ionic repulsion, leading to a higher MGC and longer time for the gel formation.

Field emission scanning electron microscopy (FESEM) was employed to examine the size and morphology of the self-assembled nanostructures formed by FmocY-Azo at different pH values. FESEM images were recorded for the lyophilized hydrogel samples (Fig. 3(d) and (e), Fig. S8), showing fibrillar morphology for all hydrogel samples. At acidic pH, the fibres appeared straight and several micrometres long, while shorter fibres were observed at higher pH values. These morphological differences supported the longer gelation times at higher pH due to the formation of shorter fibres. The fibrillar structures can be attributed to the self-assembly of FmocY-Azo, driven by π–π stacking interactions among the azobenzene groups and hydrogen bonding involving the amide and phenolic hydroxyl groups. However, the variations in morphology confirmed the differences in the molecular arrangement of FmocY-Azo at different pH values.

At room temperature, the optimal conditions were chosen for the preparation of the FmocY-Azo hydrogel (conc. = 5.0 mM in PBS buffer solution of pH = 5) for further studies. The fibrillar morphology of the hydrogel was observed from transmission electron microscopy (TEM) micrographs. Long dispersed nanofibers of several μm length and ~90 nm width were observed (Fig. 3f and Fig. S9). Development of the fibrous hydrogel network was monitored using confocal laser scanning

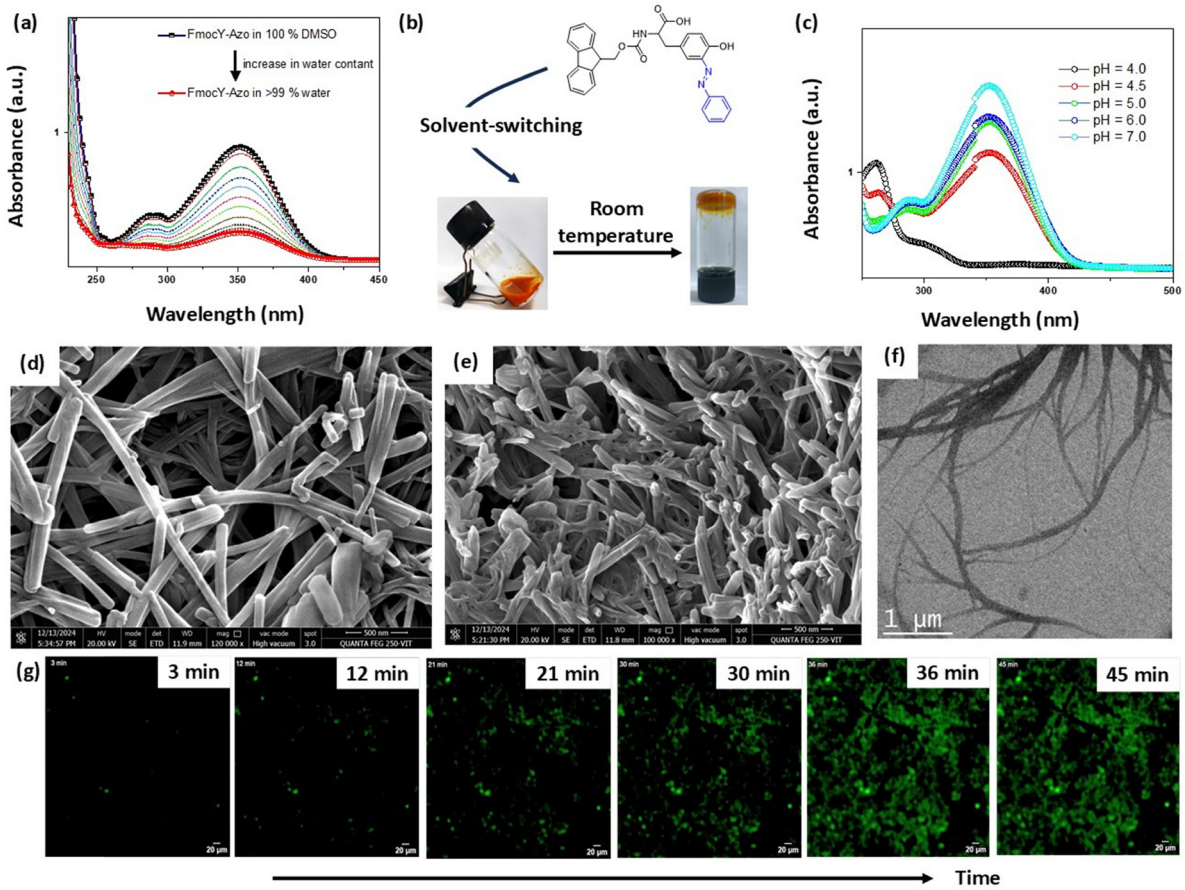


Fig. 3 Hydrogelation of FmocY-Azo. (a) Aggregation of FmocY-Azo with increasing water content. UV-vis spectra were recorded in DMSO (black circle), and with increasing the amount of water in the solution, (b) photograph of the hydrogel material prepared in PBS buffer of pH = 5 by the solvent-switching method, (c) UV-vis spectra of FmocY-Azo in PBS of different pH values, (d) and (e) FESEM micrographs of the hydrogel (d) at pH = 5 and (e) at pH = 6. The scale bar is 500 nm. (f) TEM micrographs of the hydrogel at pH = 5. The scale bar is 1 μm. (g) CLSM micrographs showing temporal evolution of fibrillar formation and hydrogel network development from the aqueous suspension of FmocY-Azo. Fluorescein (conc. = $1 \times 10^{-7}$ M) was used as the fluorophore ($\lambda_{exc.}$ = 480 nm). The scale bar is 20 μm.

microscopy (CLSM) at pH = 5 using fluorescein as a probe (conc. = $1 \times 10^{-7}$ M, $\lambda_{exc.}$ = 480 nm). The CLSM data revealed *in situ* formation of a fibrous hydrogel network over time (Fig. 3g). Fiber evolution was monitored by measuring the fluorescence intensity from the probe, which correlated with the local fiber density (Video S1 and Fig. S10). The intensity steadily increased over the first 36 minutes and then plateaued, indicating progressive network growth followed by structural stabilization. The viscoelastic properties of the hydrogel were investigated using oscillatory rheology. The storage modulus ($G'$) was greater than the loss modulus ($G''$) at lower strain values, indicating dominant elastic characteristics of the hydrogel material with the linear viscoelastic region lasting up to ~5% strain (Fig. 4a). The maximum $G'$ value was recorded as 7.6 kPa. The frequency sweep was performed at 0.1% strain for the hydrogel, showing $G'$ is independent of the applied frequencies up to ~100 rad $s^{-1}$ (Fig. 4b). Additionally, the hydrogel exhibited thermo-reversible behaviour at pH 5. At higher temperature (~90 °C), the hydrogel transitioned to a sol, which reverted to a hydrogel upon cooling (Fig. 4c, top panel). The material also demonstrated thixotropic properties at pH 5, behaving as a fluid under mechanical agitation and reforming into a hydrogel once the stress was removed (Fig. 4c, bottom panel). For these experiments, the hydrogels were prepared using the solvent-switching method (10 mM, in pH = 5 buffer solution), then mechanically shaken and left undisturbed for ~5 hours to allow recovery (Table S3). To further investigate thixotropy at pH 5, rheological measurements were conducted using a rheometer (Fig. 4d). A time sweep experiment was performed at low strain (0.1%) and high strain (50% for 10 min) at a constant frequency of 6 rad $s^{-1}$. First, the gel formation process, induced by solvent switching, was monitored through the time-dependent evolution of $G'$. The increase in $G'$ over time confirmed progressive gel formation. At low strain (0.1%), $G'$ was higher than $G''$, indicating the hydrogel state. However, upon applying high strain (50%), $G''$ surpassed $G'$, consistent with a gel-to-sol transition. Interestingly, with the release of strain, gel reformation occurred, as evidenced by $G'$ once again exceeding $G''$. The gel strength recovered after ~4.5 h, which is consistent with the vial-inversion test.

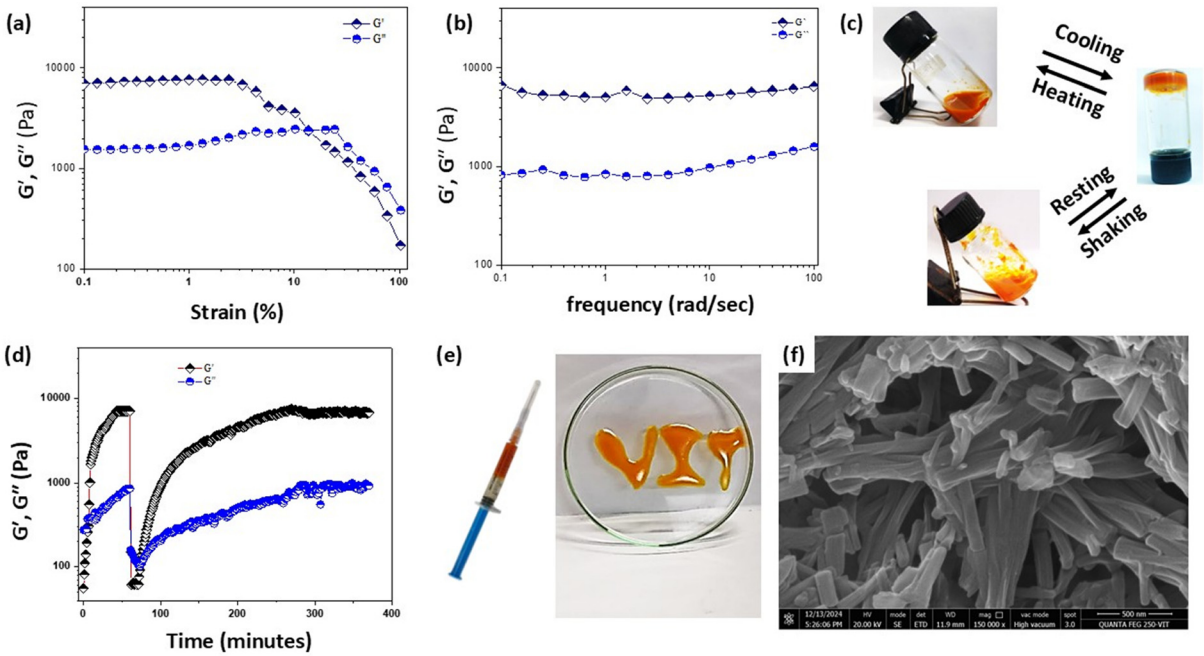


Fig. 4 Properties of FmocY-Azo hydrogelation. (a) and (b) Rheology measurement of the gel prepared at pH = 5: (a) strain sweep performed at 6 rad $s^{-1}$, (b) frequency sweep performed at 0.1% strain, (c) photographs of the thermo-reversible hydrogelation (top panel) and thixotropic behaviour (bottom panel) of FmocY-Azo prepared in a buffer solution of pH = 5. The sol is obtained at high temperature or under mechanical stress, whereas the hydrogel reformed upon cooling or under resting conditions, (d) the thixotropic properties of the FmocY-Azo hydrogel prepared at pH = 5 under the application and release of shear strain, (e) injectability: a hydrogel formed by FmocY-Azo can be easily extruded through a syringe to create defined patterns, demonstrating clear injectability, and (f) FESEM micrograph of the hydrogel that formed after removing mechanical stress. The scale bar is 500 nm.

Moreover, the hydrogels formed by FmocY-Azo could be easily extruded through a syringe to create patterned text (Fig. 4e), highlighting their potential utility in release systems.[44] FESEM imaging of the reformed hydrogel after the removal of stress revealed the fibrillar morphology (Fig. 4f), confirming the reversible structural transition. The thixotropic behaviour was also observed for the hydrogel prepared at pH 6, while the hydrogels prepared at other pH values did not exhibit this property.

### 3.4 Light-responsive behaviour

Next, we examined the light-responsiveness of the FmocY-Azo hydrogel. Upon light irradiation, the azobenzene functionality underwent *trans* → *cis* isomerization that can disrupt the π–π stacking interaction and favour the hydrogel → sol transition. Indeed, the hydrogel (5.0 mM conc. in PBS buffer of pH = 5) transformed to a pale-yellow viscous solution upon 370 nm light irradiation (intensity: 100 W $cm^{-2}$ at room temperature) without any mechanical stimulation (Fig. 5a). The FESEM image of the hydrogel reformed ∼12 h after light exposure showed reappearance of a fibrillar network (Fig. 5b). However, these regenerated fibrils were noticeably shorter and more aggregated, indicating a less controlled self-assembly process. Besides, the time taken for the hydrogel → sol transition depends on the hydrogelator concentration – for example, conversion required 30 minutes for the hydrogel prepared from 5.0 mM of FmocY-Azo, whereas gelation required more than 3 hours for the hydrogel prepared from 6.5 mM of FmocY-Azo (Table S4, SI). The hydrogel formed by FmocY-Azo can be employed for controlled cargo release.[24,25,44] The hydrogel matrix of FmocY-Azo can entrap cargo molecules (drugs, proteins, and vitamins) within its structure and allow release of the cargo *via* light-induced supramolecular hydrogel network erosion.

### 3.5 Photo-controlled $VB_{12}$ release

Vitamin $B_{12}$ ($VB_{12}$, cyanocobalamin) is an essential nutrient characterized by its low bioavailability. Cobalt deficiency in humans is treated using controlled-release $VB_{12}$ formulations that enhance cobalt concentration in blood serum and liver.[45] Controlled release of vitamin $B_{12}$ is reported in the literature, predominantly achieved using polymeric hydrogels that respond to pH changes or temperature variations.[46,47] Light-induced controlled release of $VB_{12}$ from the polymeric hydrogel matrix is rarely reported,[48] whereas light controlled release of $VB_{12}$ from the supramolecular hydrogel matrix is not reported. We choose $VB_{12}$ as the model cargo molecule to encapsulate within the FmocY-Azo hydrogel network for its controlled release *via* light irradiation (Fig. 5c). We mixed $VB_{12}$ (0.1 mM in water) with FmocY-Azo and followed the hydrogelation procedure using the solvent-switching method (in PBS buffer, pH = 5). The $VB_{12}$-entrapped hydrogel was obtained after the mixture was left undisturbed at room temperature for a sufficient time (∼2 h), which was confirmed by the vial inversion test. The $VB_{12}$-entrapped FmocY-Azo hydrogel exhibited a higher MGC (minimum gelation concentration) and slower

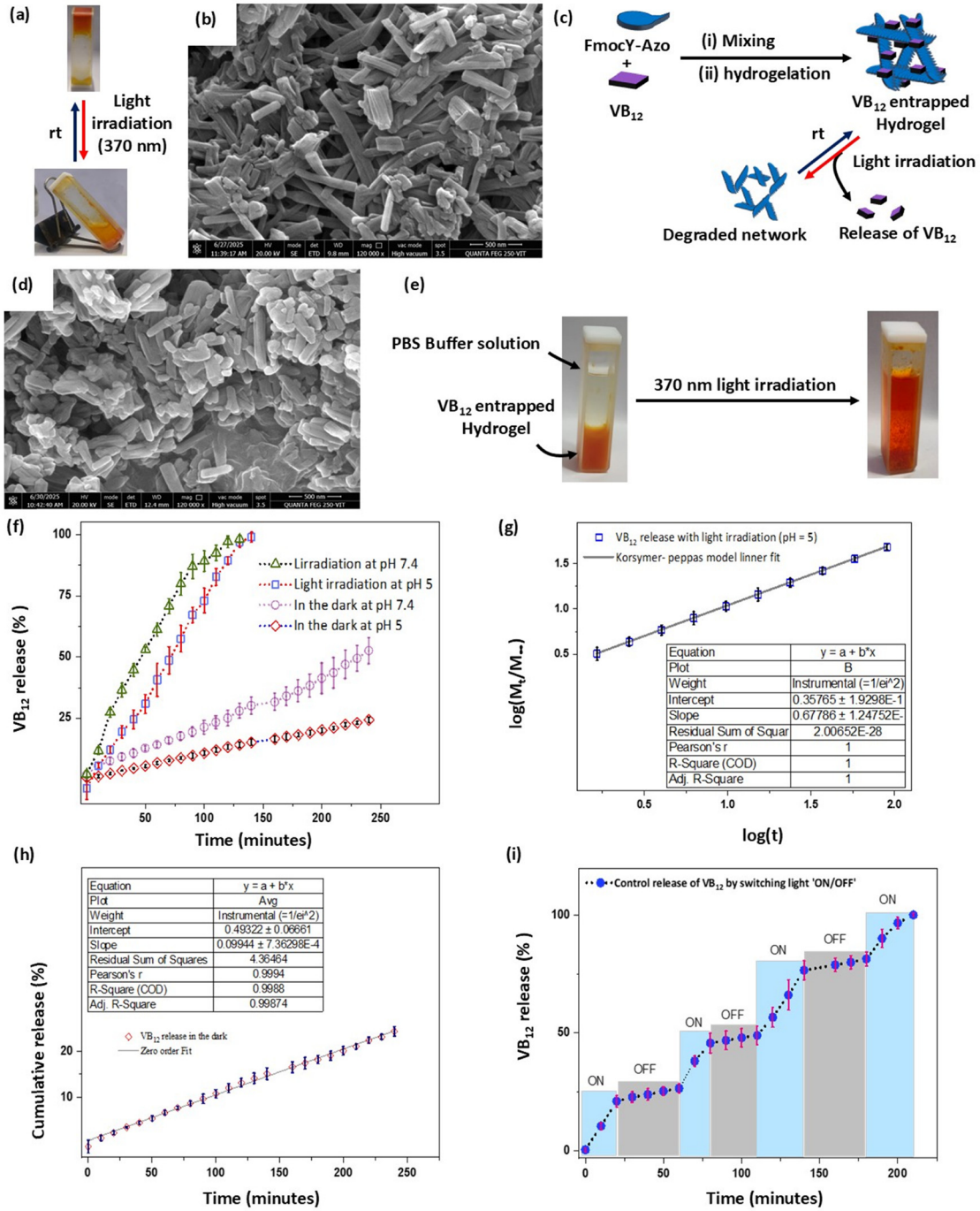


Fig. 5 Light-triggered hydrogel erosion. (a) A photograph showing the hydrogel → sol transition under light irradiation and sol → hydrogel re-conversion at room temperature in the dark. (b) FESEM micrograph of the re-formed hydrogel at room temperature after ceasing light irradiation. The scale bar is 500 nm. (c) A cartoon representation of $VB_{12}$-entrapped FmocY-Azo hydrogel preparation and light-induced $VB_{12}$ release from the hydrogel network. (d) FESEM image of the $VB_{12}$-entrapped FmocY-Azo hydrogel. The scale bar is 500 nm. (e) Photograph of the $VB_{12}$ loaded FTy-Azo hydrogel (at the bottom of the cuvette) and added buffer solution (on top of the cuvette) and photograph of the cuvette after the release of $VB_{12}$ under 370 nm UV light irradiation. (f) Release profile of $VB_{12}$ at pH 5 in the presence (open square) and absence (open diamond) of light irradiation and release profile of $VB_{12}$ at pH 7.4 in the presence (open triangle) and absence (open circle) of light irradiation. (g) Kinetic analysis of $VB_{12}$ release from the hydrogel at pH 5 in buffer media with light irradiation. The solid line represents the fitted release according to the Korsmeyer–Peppas kinetic model. (h) Kinetic analysis of $VB_{12}$ release from the hydrogel at pH 5 in the dark. The solid line represents the fitted release according to a zero-order kinetic model. (i) 'On-demand' release of VB12 from the hydrogel by switching light irradiation 'ON' and 'OFF' at pH = 5. Markers indicate the experimental data, and error bars are based on standard errors in triplicate runs. The dotted lines are to guide the eye.

gelation kinetics (Table S5). This can be ascribed to the hydrophilic, bulky $VB_{12}$ molecules interfering with the packing of fibrillar hydrogelators.[47,49] The FESEM image supported the longer gelation times due to the formation of shorter fibres. The prolonged gelation time and higher MGC were supported by the FESEM micrograph of the $VB_{12}$-entrapped FmocY-Azo hydrogel, showing short fibers (Fig. 5d). To examine the release profile, PBS buffer solution (1.7 ml, pH = 5.0) was added over the hydrogel material and the release of $VB_{12}$ was monitored by UV-vis spectroscopy by carefully collecting an aliquot (1.0 mL) from the top of the hydrogel and an equal volume of PBS buffer (1.0 mL) was added to maintain a constant volume (Fig. 5e). The amount of released material was estimated from UV-vis spectra following the absorbance at 550 nm for $VB_{12}$, and the absorbance was compared with the standard curve of $VB_{12}$ (Fig. S11). In the dark, only 25% $VB_{12}$ was released from the hydrogel matrix over 4 hours (Fig. 5f, red diamond). In contrast, 100% release of $VB_{12}$ was observed within 2 hours in the presence of light irradiation (Fig. 5f, blue square).

The release profile was also assessed under physiologically relevant conditions (pH 7.4). $VB_{12}$-loaded hydrogels were prepared *via* the solvent-switching method in PBS buffer of pH 7.4 (Table S6). In the dark, $\sim$52% of $VB_{12}$ was released over 4 hours (Fig. 5f, purple circle), indicating a higher passive release rate compared to pH 5.0. This increased release is attributed to a weaker gel network at pH 7.4, likely due to electrostatic repulsion among the deprotonated ionizable groups (–COOH) present in FmocY-Azo.[50] Consistent with this observation, the minimum gelation concentration increased to 6.3 mM at pH 7.4 (Table S1), compared to 5.0 mM at pH 5.0. Rheological analysis further confirmed the reduced gel strength at pH 7.4, with a maximum storage modulus ($G'$) of 0.2 kPa, significantly lower than the 7.6 kPa observed at pH 5.0 (Fig. S12). However, under light irradiation, rapid release of $VB_{12}$ ($\sim$98%) was achieved within 2 hours (Fig. 5f), confirming the robust photoresponsive behaviour of the hydrogel under physiological conditions.

The release of $VB_{12}$ from the hydrogel formed by FmocY-Azo was further examined based on the four mathematical models used to describe drug release from various pharmaceutical formulations:[51,52] zero-order model, first-order model, Higuchi model, and Korsmeyer–Peppas model (Table S7). The obtained data from the mentioned models were fitted and evaluated according to the correlation coefficient $R^2$ (Fig. S13 and S14 for pH 5). For the better fit of the data to the model, we consider a higher $R^2$ value (approaching 1), suggesting its suitability for the analysis (Table S8 for pH 5). At pH 5, we found that the release of $VB_{12}$ in the presence of light irradiation followed the Korsmeyer–Peppas model with $R^2$ = 1 (Fig. 5g). In contrast, the release followed the zero-order model with $R^2$ = 0.9987 in the dark (Fig. 5h). These findings suggested a constant release of $VB_{12}$ in the dark due to the diffusion mechanism. However, a non-Fickian law of diffusion was followed in the presence of light, indicating light-induced degradation of the hydrogel matrix for the release of $VB_{12}$.

Next, we examined the 'on-demand' release kinetics of $VB_{12}$ from the hydrogel matrix by switching light 'ON/OFF'. At pH 5, we observed $\sim$25.0% $VB_{12}$ release by light irradiation for the first 20 minutes, whereas only $\sim$2.5% release was observed for the next 40 minutes in the dark (Fig. 5i). Likewise, faster release of $VB_{12}$ from the hydrogel matrix was observed upon light irradiation (switch 'ON'), whereas the release of $VB_{12}$ was significantly slower in the dark (switch 'OFF'). These results collectively demonstrate that the on-demand release of $VB_{12}$ can be achieved by alternating light irradiation 'ON/OFF', demonstrating the potential for precise modulation of cargo delivery.

## 4. Conclusions

In summary, we designed and synthesized a novel light responsive hydrogelator (FmocY-Azo) *via* a one-pot reaction that proceeded with good yield. The hydrogelator displayed reversible *trans–cis* isomerization *via* light irradiation, and thermal back isomerization in the dark at room temperature. In aqueous media, FmocY-Azo showed self-assembly *via* π–π interactions. Solvent switching in PBS buffer medium provided a supramolecular hydrogel material under ambient conditions. We demonstrated that FmocY-Azo formed a stable hydrogel in the pH range 5–8 *via* the formation of a fibrous network. The pH of the solution significantly influences the self-assembly of the hydrogelator by optimising π–π interactions, hydrogen bonding interactions, and ionic interactions. The hydrogel displayed thermo-responsive and thixotropic properties. In addition, the hydrogel undergoes hydrogel-to-sol conversion upon light irradiation. The hydrogel can be used as a vitamin carrier that would allow accelerated release of vitamin $B_{12}$ upon light irradiation. Additionally, precise control of cargo release from the hydrogel can be obtained by switching light 'ON/OFF'. The insight that a simple photoswitchable hydrogelator enabling supramolecular hydrogelation *via* self-assembly under ambient conditions and light-induced controlled release of the cargo by disassembly would aid the design of 'smart' materials and systems with interesting properties for various biomedical applications.[53]

## Author contributions

C. M. conceived the idea. D. C. and C. M. designed and performed the experiments, analysed the data, and wrote the manuscript. C. M. supervised the research. All authors commented on the manuscript and have given approval to the final version of the manuscript.

## Conflicts of interest

A part of this work has been filed as an Indian patent application (Application No. 202541039265) with all authors as inventors.

## Data availability

The authors declare that the data supporting the findings of this study are available within the paper and its supplementary information (SI). Supplementary information is available. See DOI: https://doi.org/10.1039/d5ma00736d.

Should any raw data files be needed in another format, they are available from the corresponding author upon reasonable request.

## Acknowledgements

C. M. acknowledges the funding from VIT through a seed grant (no. SG20240013). The authors thank Prof. Amit Kumar Jaiswal and Mr Aditya Ravindra Kadam (CBCMT, VIT) for assistance with rheological measurements. The authors also acknowledge Prof. Pratheepkumar Annamalai and Prof. Arup Sinha (Department of Chemistry, VIT) for providing access to the light chamber and UV-vis spectrometer. All authors acknowledge the central instrumental facility of VIT Vellore for supporting this work.

## References

1 D. Philp and J. F. Stoddart, Self-assembly in natural and unnatural systems, *Angew. Chem. Int. Ed.*, 1996, **35**, 1154–1196, DOI: 10.1002/anie.199611541.
2 S. Zhang, Emerging biological materials through molecular self-assembly, *Biotechnol. Adv.*, 2002, **20**, 321–339, DOI: 10.1016/S0734-9750(02)00026-5.
3 X. Liu, X. Sun and G. Liang, Peptide-based supramolecular hydrogels for bioimaging applications, *Biomater. Sci.*, 2021, **9**, 315–327, DOI: 10.1039/D0BM01020K.
4 B. Xie, Y. F. Ding, M. Shui, L. Yue, C. Gao, I. W. Wyman and R. Wang, Supramolecular biomaterials for bio-imaging and imaging-guided therapy, *Eur. J. Nucl. Med. Mol. Imaging*, 2022, **49**, 1200–1210, DOI: 10.1007/s00259-021-05622-7.
5 R. Luo, X. Xiang, Q. Jiao, H. Hua and Y. Chen, Photoresponsive hydrogels for tissue engineering, *ACS Biomater. Sci. Eng.*, 2024, **10**, 3612–3630, DOI: 10.1021/acsbiomaterials.4c00314.
6 Y. Li, C. Shao, Z. Pei and Y. Pei, Recent advancements of nanostructured surface-specific supramolecular assemblies and their application in biomedical engineering, *Green Chem.*, 2025, **27**, 1871–1894, DOI: 10.1039/D4GC04889J.
7 F. Trausel, F. Versluis, C. Maity, J. M. Poolman, M. Lovrak, J. H. Van Esch and R. Eelkema, Catalysis of supramolecular hydrogelation, *Acc. Chem. Res.*, 2016, **49**, 1440–1447, DOI: 10.1021/acs.accounts.6b00137.
8 D. K. Smith, Supramolecular gels–a panorama of low-molecular-weight gelators from ancient origins to next-generation technologies, *Soft Matter*, 2024, **20**, 10–70, DOI: 10.1039/D3SM01301D.
9 A. Levin, T. A. Hakala, L. Schnaider, G. J. L. Bernardes, E. Gazit and T. P. J. Knowles, Biomimetic peptide self-assembly for functional materials, *Nat. Chem. Rev.*, 2020, **4**, 615–634, DOI: 10.1038/s41570-020-0215.
10 J. Lee, M. Ju, O. H. Cho, Y. Kim and K. T. Nam, Tyrosine-rich peptides as a platform for assembly and material synthesis, *Adv. Sci.*, 2018, **6**, 1801255, DOI: 10.1002/advs.201801255.
11 P. Chakraborty and E. Gazit, Amino acid based self-assembled nanostructures: Complex structures from remarkably simple building blocks, *ChemNanoMat*, 2018, **4**, 730–740, DOI: 10.1002/cnma.201800147.
12 D. Bharathidasan and C. Maity, Self-assembly of tyrosine scaffolds in aqueous media: Complex molecular architectures from simple building blocks, *Chem. Rec.*, 2025, **25**, e202500005, DOI: 10.1002/tcr.202500005.
13 M. Hou and S. Liu, Recent progress of pH-responsive peptides, polypeptides, and their supramolecular assemblies for biomedical applications, *Biomacromolecules*, 2024, **25**, 5402–5416, DOI: 10.1021/acs.biomac.4c00688.
14 S. Xian and M. J. Webber, Temperature-responsive supramolecular hydrogels, *J. Mater. Chem. B*, 2020, **8**, 9197–9211, DOI: 10.1039/D0TB01814G.
15 L. Li, J. M. Scheiger and P. A. Levkin, Design and applications of photoresponsive hydrogels, *Adv. Mater.*, 2019, **31**, 1807333, DOI: 10.1002/adma.201807333.
16 M. Vázquez-González and I. Willner, Stimuli-responsive biomolecule-based hydrogels and their applications, *Angew. Chem. Int. Ed.*, 2020, **59**, 15342–15377, DOI: 10.1002/anie.201907670.
17 X. Wang and Q. Wang, Enzyme-laden bioactive hydrogel for biocatalytic monitoring and regulation, *Acc. Chem. Res.*, 2021, **54**, 1274–1287, DOI: 10.1021/acs.accounts.0c00832.
18 H. R. Culver, J. R. Clegg and N. A. Peppas, Analyte-responsive hydrogels: Intelligent materials for biosensing and drug delivery, *Acc. Chem. Res.*, 2017, **50**, 170–178, DOI: 10.1021/acs.accounts.6b00533.
19 P. R. A. Chivers and D. K. Smith, Shaping and structuring supramolecular gels, *Nat. Rev. Mater.*, 2019, **4**, 463–478, DOI: 10.1038/s41578-019-0111-6.
20 Z. H. Liao and F. Wang, Light-controlled smart materials: Supramolecular regulation and applications, *Smart Mol.*, 2024, **2**, e20240036, DOI: 10.1002/smo.20240036.
21 M. Younis, S. Ahmad, A. Atiq, M. A. Farooq, M. H. Huang and M. Abbas, Recent progress in azobenzene-based supramolecular materials and applications, *Chem. Rec.*, 2023, **23**, e202300126, DOI: 10.1002/tcr.202300126.
22 W. A. Velema, M. C. A. Stuart, W. Szymanski and B. L. Feringa, Light-triggered self-assembly of a dichromonyl compound in water, *Chem. Commun.*, 2013, **49**, 5001, DOI: 10.1039/c3cc41018h.
23 X. Xiao, J. Hu, X. Wang, L. Huang, Y. Chen, W. Wang, J. Li and Y. Zhang, A dual-functional supramolecular hydrogel based on a spiropyran–galactose conjugate for target-mediated and light-controlled delivery of microRNA into cells, *Chem. Commun.*, 2016, **52**, 12517–12520, DOI: 10.1039/C6CC07386G.
24 D. Wang, M. Wagner, H. J. Butt and S. Wu, Supramolecular hydrogels constructed by red-light-responsive host–guest interactions for photo-controlled protein release in deep tissue, *Soft Matter*, 2015, **11**, 7656–7662, DOI: 10.1039/C5SM01888A.

25 J. Karcher, S. Kirchner, A. L. Leistner, C. Hald, P. Geng, T. Bantle, P. Gödtel, J. Pfeifer and Z. L. Pianowski, Selective release of a potent anticancer agent from a supramolecular hydrogel using green light, *RSC Adv.*, 2021, **11**, 8546–8551, DOI: **10.1039/D0RA08893E**.

26 F. A. Larik, L. L. Fillbrook, S. S. Nurttila, A. D. Martin, R. P. Kuchel, K. A. Taief, M. Bhadbhade, J. E. Beves and P. Thordarson, Ultra-low molecular weight photoswitchable hydrogelators, *Angew. Chem. Int. Ed.*, 2021, **60**, 6764–6770, DOI: **10.1002/anie.202015703**.

27 F. Xu and B. L. Feringa, Photoresponsive supramolecular polymers: From light-controlled small molecules to smart materials, *Adv. Mater.*, 2023, **35**, 2204413, DOI: **10.1002/adma.202204413**.

28 F. Gao, X. Yang and W. Song, Bioinspired supramolecular hydrogel from design to applications, *Small Methods*, 2024, **8**, 2300753, DOI: **10.1002/smtd.202300753**.

29 T. A. Shell and D. S. Lawrence, Vitamin $B_{12}$: A tunable, long wavelength, light-responsive platform for launching therapeutic agents, *Acc. Chem. Res.*, 2015, **48**(11), 2866–2874, DOI: **10.1021/acs.accounts.5b00331**.

30 Y. Huang, Z. Qiu, Y. Xu, J. Shi, H. Lin and Y. Zhang, Supramolecular hydrogels based on short peptides linked with conformational switch, *Org. Biomol. Chem.*, 2011, **9**, 2149–2155, DOI: **10.1039/c0ob01057j**.

31 M. E. Roth-Konforti, M. Comune, M. Halperin-Sternfeld, I. Grigoriants, D. Shabat and L. Adler-Abramovich, UV light–responsive peptide-based supramolecular hydrogel for controlled drug delivery, *Macromol. Rapid Commun.*, 2018, **39**, e1800588, DOI: **10.1002/marc.201800588**.

32 C. Guilbaud-Chéreau, B. Dinesh, R. Schurhammer, D. Collin, A. Bianco and C. Ménard-Moyon, Protected amino acid–based hydrogels incorporating carbon nanomaterials for near-infrared irradiation-triggered drug release, *ACS Appl. Mater. Interfaces*, 2019, **11**, 13147–13157, DOI: **10.1021/acsami.9b02482**.

33 W. Xiong, H. Zhou, C. Zhang and H. Lu, An amino acid-based gelator for injectable and multi-responsive hydrogel, *Chin. Chem. Lett.*, 2017, **28**, 2125–2128, DOI: **10.1016/j.cclet.2017.09.019**.

34 S. Koide and S. S. Sidhu, The importance of being tyrosine: Lessons in molecular recognition from minimalist synthetic binding proteins, *ACS Chem. Biol.*, 2009, **4**, 325–334, DOI: **10.1021/cb800314v**.

35 E. R. Draper, K. L. Morris, M. A. Little, J. Raeburn, C. Colquhoun, E. R. Cross, T. O. McDonald, L. C. Serpell and D. J. Adams, Hydrogels formed from Fmoc amino acids, *CrystEngComm*, 2015, **17**, 8047–8057, DOI: **10.1039/C5CE00801H**.

36 D. Bharathidasan, A. S. Salvi, S. Bose and C. Maity, Biochemical Signal-Induced Supramolecular Hydrogelation for Structured Free-Standing Soft Material Formation, *Macromol. Biosci.*, 2024, **24**, e2400419, DOI: **10.1002/mabi.202400419**.

37 H. M. D. Bandara and S. C. Burdette, Photoisomerization in different classes of azobenzene, *Chem. Soc. Rev.*, 2012, **41**, 1809–1825, DOI: **10.1039/C1CS15179G**.

38 S. Steinwand, T. Halbritter, D. Rastädter, J. M. Ortiz-Sánchez, I. Burghardt, A. Heckel and J. Wachtveitl, Ultrafast spectroscopy of hydroxy-substituted azobenzenes in water, *Chem. – Eur. J.*, 2015, **21**, 15720–15731, DOI: **10.1002/chem.201501863**.

39 J. García-Amorós and D. Velasco, Recent advances towards azobenzene-based light-driven real-time information-transmitting materials, *Beilstein J. Org. Chem.*, 2012, **8**, 1003–1017, DOI: **10.3762/bjoc.8.113**.

40 A. Natansohn and P. Rochon, Photoinduced motions in azo-containing polymers, *Chem. Rev.*, 2002, **102**, 4139–4176, DOI: **10.1021/cr970155y**.

41 D. M. Ryan, S. B. Anderson, F. T. Senguen, R. E. Youngman and B. L. Nilsson, Self-Assembly and hydrogelation promoted by $F_5$-phenylalanine, *Soft Matter*, 2010, **6**, 475–479, DOI: **10.1039/B916738B**.

42 R. E. Ginesi and E. R. Draper, Methods of changing low molecular weight gel properties through gelation kinetics, *Soft Matter*, 2024, **20**, 3887–3896, DOI: **10.1039/D4SM00238E**.

43 A. A. Beharry, O. Sadovski and G. A. Woolley, Azobenzene photoswitching without ultraviolet light, *J. Am. Chem. Soc.*, 2011, **133**, 19684–19687, DOI: **10.1021/ja209239m**.

44 W. Yang, J. Chen, Z. Zhao, M. Wu, L. Gong, Y. Sun, C. Huang, B. Yan and H. Zeng, Recent advances in fabricating injectable hydrogels via tunable molecular interactions for bio-applications, *J. Mater. Chem. B*, 2024, **12**, 332–349, DOI: **10.1039/D3TB02105J**.

45 A. Pettenuzzo, R. Pigot and L. Ronconi, Vitamin $B_{12}$-metal conjugates for targeted chemotherapy and diagnosis: Current status and future prospects, *Eur. J. Inorg. Chem.*, 2017, 1625–1638, DOI: **10.1002/ejic.201601217**.

46 B. Maheswari, P. E. J. Babu and M. Agarwal, Role of N-vinyl-2-pyrrolidinone on the thermoresponsive behavior of PNIPAm hydrogel and its release kinetics using dye and vitamin-$B_{12}$ as model drug, *J. Biomater. Sci., Polym. Ed.*, 2014, **25**, 269–286, DOI: **10.1080/09205063.2013.854149**.

47 D. Kundu and T. Banerjee, Carboxymethyl cellulose–xylan hydrogel: Synthesis, characterization, and in vitro release of vitamin $B_{12}$, *ACS Omega*, 2019, **4**, 4793–4803, DOI: **10.1021/acsomega.8b03671**.

48 X. Cao, X. Peng, L. Zhong and R. Sun, Multiresponsive hydrogels based on xylan-type hemicelluloses and photoisomerized azobenzene copolymer as drug delivery carrier, *J. Agric. Food Chem.*, 2014, **62**, 10000–10007, DOI: **10.1021/jf504040s**.

49 M. H. Kim, H. Park, J. Y. Shin and W. H. Park, Effect of vitamin derivatives on gelation rate and gel strength of methylcellulose, *Carbohydr. Polym.*, 2018, **196**, 414–421, DOI: **10.1016/j.carbpol.2018.05.042**.

50 S. Sutton, N. L. Campbell, A. I. Cooper, M. Kirkland, W. J. Frith and D. J. Adams, Controlled release from modified amino acid hydrogels governed by molecular size or network dynamics, *Langmuir*, 2009, **25**, 10285, DOI: **10.1021/la9011058**.

51 M. Askarizadeh, N. Esfandiari, B. Honarvar, S. A. Sajadian and A. Azdarpour, Kinetic modeling to explain

the release of medicine from drug delivery systems, *ChemBioEng Rev.*, 2023, **10**, 1006–1049, DOI: **10.1002/cben.202300027**.

52 C. Harkos, A. G. Hadjigeorgiou, C. Voutouri, A. S. Kumar, T. Stylianopoulos and R. K. Jain, Using mathematical modelling and AI to improve delivery and efficacy of therapies in cancer, *Nat. Rev. Cancer*, 2025, **25**, 324–340, DOI: **10.1038/s41568-025-00796-w**.

53 B. Cecen, S. Hassan, X. Li and Y. S. Zhang, Smart biomaterials in biomedical applications: Current advances and possible future directions, *Macromol. Biosci.*, 2024, **24**, 2200550, DOI: **10.1002/mabi.202200550**.